*mathematics*

MDPI

*Article*

# Enhancing Diversity and Convergence in MMOPs with a Gaussian Similarity-Based Evolutionary Algorithm

**Shizhao Wei [1] and Da-Jung Cho [2,*]**

[1] Department of Artificial Intelligence, Ajou University, 206, World cup-ro, Yeongtong-gu, Suwon-si 16499, Republic of Korea; weishizhao@ajou.ac.kr
[2] Department of Software and Computer Engineering, Ajou University, 206, World cup-ro, Yeongtong-gu, Suwon-si 16499, Republic of Korea
* Correspondence: dajungcho@ajou.ac.kr

**Abstract:** Multi-modal multi-objective optimization problems (MMOPs) are challenging due to multiple solutions sharing similar objective values. Existing algorithms for solving MMOPs typically evaluate the crowding in the decision space and objective space independently, leading to an imbalance in diversity between the two spaces. We introduce a mechanism that balances diversity in both the decision and objective spaces, aiming to enhance diversity while maintaining convergence in both spaces. We propose a multi-modal multi-objective evolutionary algorithm (MMEA) that selects qualified solutions based on Gaussian similarity. Gaussian similarity assesses the closeness of solution pairs and serves as the diversity fitness criterion for the algorithm. We conducted experiments on 28 benchmark problems and compared MMEA-GS with five state-of-the-art approaches. The results demonstrate that MMEA-GS effectively addresses most MMOPs, achieving higher diversity and convergence.

**Keywords:** multi-objective optimization; multi-modal optimization problems; evolutionary algorithms; Gaussian similarity; diversity fitness

**MSC:** 68W50



Received: 1 January 2025
Revised: 14 January 2025
Accepted: 17 January 2025
Published: 18 January 2025

**Citation:** Wei, S.; Cho, D.-J. Enhancing Diversity and Convergence in MMOPs with a Gaussian Similarity-Based Evolutionary Algorithm. *Mathematics* **2025**, *13*, 308. https://doi.org/10.3390/math13020308

**Copyright:** © 2025 by the authors. Licensee MDPI, Basel, Switzerland. This article is an open access article distributed under the terms and conditions of the Creative Commons Attribution (CC BY) license (https://creativecommons.org/licenses/by/4.0/).

## 1. Introduction

Multi-objective optimization problems (MOPs) are extensively studied in fields such as economics and finance [1], energy management [2], manufacturing and industrial processes [3], and healthcare [4]. The primary goal is to identify a set of solutions in the decision space that correspond to optimal objective values in the objective space [5–7]. When dealing with multiple objective functions, particularly conflicting ones, it is often impossible to achieve a single solution that optimally satisfies all objectives simultaneously. For instance, portfolio optimization problems illustrate this challenge, as the objectives of maximizing returns and minimizing risk inherently conflict with each other. Therefore, finding the trade-off among the multiple objective functions is the challenge of the MOPs. Pareto optimality defines the set of best trade-off solutions that balance the values of the objective functions [8]. The Pareto set (PS) represents the set of optimal trade-off solutions in the decision space, while the Pareto front (PF) represents the corresponding objective values of the PS in the objective space.

Multi-objective optimization evolutionary algorithms (MOEAs) have been proposed to solve MOPs effectively [9]. In general, the pursuit of identifying a set of solutions

with good convergence and diversity are two of the primary goals in the MOEAs community [10]. For the convergence, some MOEAs such as strength Pareto evolutionary algorithm (SPEA) [11], SPEA-II [12], and Pareto envelope-based selection algorithm II [13] introduce and develop the Pareto dominant relationship as an efficient technique to achieve a better approximation to the PF. However, the Pareto dominant relationship is unable to guarantee a diverse set of solutions, which suggests that the distribution of solutions in the decision space has received only limited attention from the MOEA community. Nevertheless, the necessity of ensuring a diverse population is an arising issue that is recommended by decision makers [5]. Figure 1 illustrates an example of two objectives, where the three objective values $F(x^a), F(x^b)$, and $F(x^c)$ are crowded in a small region. This phenomenon results in similar objective values, indicating insufficient exploration of the decision space. To address this, Deb et al. [14] proposed the crowding distance approach to maintain diversity by screening the solutions with lower density in a neighboring region. Gao et al. [15] improved upon this by introducing an adaptive mechanism that adjusts the balance between convergence and diversity. This adaptive strategy dynamically adjusts how much focus should be placed on improving the quality of solutions versus exploring diverse solutions.

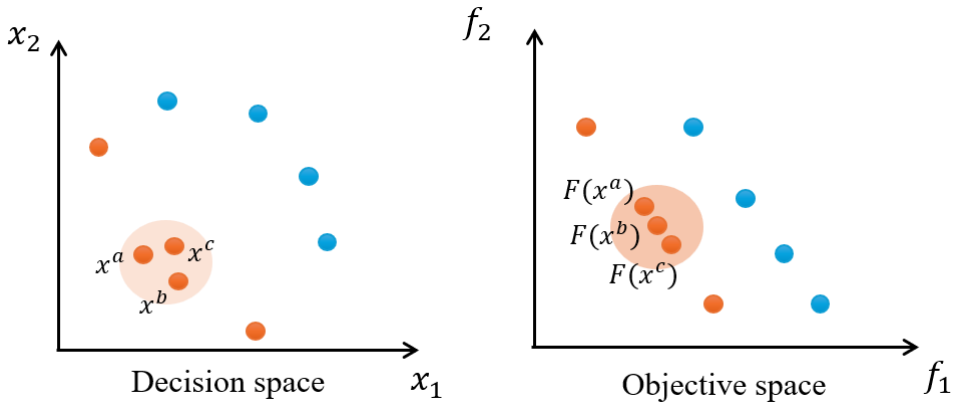



**Figure 1.** An MOP example, where the crowding of $x^a, x^b, x^c$ in the decision space cause the crowding of $F(x^a), F(x^b), F(x^c)$ in the objective space.

Multiple Pareto optimal solutions may correspond to the same objective value, a situation known as *multi-modal*. MOPs exhibiting this property are referred to as *multi-modal multi-objective optimization problems* (MMOPs). In MMOPs, multiple objective functions may overlap within continuous regions, causing feasible solutions to disappear. This means there are areas where no solutions meet the constraints or objectives, leading to a lack of feasible solutions in those regions. The collision among the objective functions results in narrow infeasible regions in the objective space. This creates gaps or separations between global optima (optimal solutions), resulting in a local Pareto front (LPF) and multiple global Pareto fronts (PFs). Real-world constraints can make the Pareto front more complex [14], potentially making it impossible to employ solutions from the global Pareto fronts in some practical scenarios. This complexity arises because, in real-world problems, constraints may make certain solutions unfeasible despite their optimality in an unconstrained setting. In cases where the global PF cannot be used due to constraints or other limitations, the LPF becomes a practical alternative for decision makers. This is an important reason for identifying and focusing on the LPF in MMOPs. Addressing MMOPs is crucial as it helps uncover the fundamental characteristics and complexities inherent in multi-objective optimization problems, providing deeper insights into their structure and challenges [16,17].

The main challenges in multi-modal multi-objective optimization problems (MMOPs) are balancing diversity both in the objective space and decision space while ensuring con-

vergence towards the Pareto set (PS) [18]. Once a small set of optimal solutions are found, the solutions quickly converge to the Pareto set, which can lead to insufficient exploration of the decision space. This means the optimization process might miss exploring other potentially optimal regions. The presence of multiple solutions in the decision space that result in the same objective value makes it difficult to have all of these solutions coexisting simultaneously. This creates a challenge in handling the diversity of the solutions. While some multi-objective evolutionary algorithms (MOEAs) have improved diversity in solving traditional MOPs, they still face difficulties in addressing the multi-modal nature of MMOPs. The standard MOEAs may not be sufficient to tackle the complexities of multiple, conflicting solutions. To overcome these challenges, a multi-modal multi-objective evolutionary algorithm (MMEA) is proposed as an enhancement to MOEAs, specifically designed to address MMOPs. Over the past decade, researchers have focused on improving the mechanisms for selecting solutions with better diversity to update the solution set. Liang et al. [19] analyzed the characteristics of MMOPs and designed DN-NSGA-II to address their challenges by introducing a crowding distance into the decision space. Liu et al. [20] improved decision space diversity using crowding distance, and Liu et al. [21] proposed TriMOEA-TA&R, which balances convergence and diversity by updating both in parallel across two archives. Li et al. [22] proposed MMEA-WI, which uses a weighted indicator to balance global and local search strategies, and Yue et al. [23] introduced MMEA-ICD, which improves search capability and convergence by incorporating Pareto rank and enhancing scaled crowding distance. This work aims to improve the balance between exploration and convergence in multi-modal multi-objective optimization. Wang et al. [24] designed MO_Ring_PSO_SCD, incorporating scaled crowding distance to balance diversity between the decision and objective spaces. Li et al. [25] introduced MMEA with the hierarchical method (HREA), using dual archives and crowding distance to maintain diversity and ensure convergence, while treating local and global optima equivalently to preserve the local Pareto set diversity.

Despite the significant progress made by existing multi-modal multi-objective evolutionary algorithms (MMEAs) in balancing diversity and convergence in both the objective and decision spaces, a major limitation persists in that crowding distance or density is calculated separately for each space. This separation can lead to biases, favoring one space over the other during the optimization process, potentially resulting in imbalances and suboptimal outcomes. To address this issue, we propose an approach using Gaussian similarity, a measurement designed to simultaneously evaluate the proximity of solutions and their corresponding objective values. By integrating Gaussian similarity into MMEA, we introduce the Multi-Modal Multi-Objective Evolutionary Algorithm with Gaussian Similarity (MMEA-GS), designed to enhance the balance between decision and objective spaces during the optimization process. The main contributions of this work are as follows:

- We introduce Gaussian similarity to simultaneously evaluate the closeness between solutions in both the decision space and the objective space. This dual consideration reduces crowding in either space, addressing a key challenge in multi-modal multi-objective optimization. It promotes a more balanced exploration of the solution space and prevents bias toward one space during the optimization process.
- We define the balanced Gaussian distance to enhance the environmental selection process by preventing the release of solutions crowded in only one space (either decision or objective space). This approach ensures that both spaces are considered when promoting diversity, leading to a more balanced distribution of solutions. It addresses the issue in traditional methods, where diversity is often increased in one space at the expense of the other.

- The MMEA-GS algorithm integrates these two components to provide an effective mechanism for calculating diversity and selecting solutions. By combining Gaussian similarity and balanced Gaussian distance, it improves the balance between convergence and diversity in both the decision and objective spaces, optimizing the overall process.

The rest of this paper is organized as follows. Section 2 provides the background on key terminologies, evolutionary algorithms, and techniques for enhancing diversity. Section 3 introduces the concept of Gaussian similarity and details each component of MMEA-GS. In Section 4, we present and discuss the results of MMEA-GS. Finally, Section 5 concludes the paper.

## 2. Background

In this section, we first provide formal definitions and terminologies. Then, we present a basic framework of evolutionary algorithms and discuss existing strategies for evaluating diversity.

### *2.1. Terminologies*

Given $m$ objective functions $f_1, f_2, \ldots, f_m$, a minimization-based multi-objective optimization problem (MOP) is defined as

$$\min F(x) = (f_1(x), f_2(x), \ldots, f_m(x)), \tag{1}$$

where $x = (x_1, \ldots, x_n)$ is a decision vector of $n$ elements in the decision space $\Omega$, and $F(x)$ is a vector of objective values corresponding to the $m$ objective functions in the objective space $R$. The primary goal of MOPs is to obtain a set of solutions that reach the Pareto optima. Multi-objective evolutionary algorithms (MOEAs) aim to increase the uniform distribution on the Pareto set (PS) while maintaining convergence. However, increasing diversity remains a significant challenge.

MOPs extend to multi-modal multi-objective optimization problems (MMOPs) when multiple solutions correspond to the same objective value, leading to multi-modal situations. An MMOP is defined as

$$\begin{aligned} &\min F(x) = (f_1(x), f_2(x), \ldots, f_m(x)) \\ &s.t.\ L_i = \{x^{I1}, \ldots, x^{Ik} | F(x^{I1}) = \cdots = F(x^{Ik}), |L_i| = k \geq 2, i \geq 1\}, \end{aligned} \tag{2}$$

where $L_i$ is the $i$-th subset of solutions of size $k$ that share the same objective value. Figure 2 illustrates an example of a bi-dimensional objective space, where the subset of solutions $L_1 = x^a, x^d, x^c, x^d$ share the objective value $F(x^a)$, and $L_2 = x^e, x^f, x^g$ share the objective value $F(x^b)$.

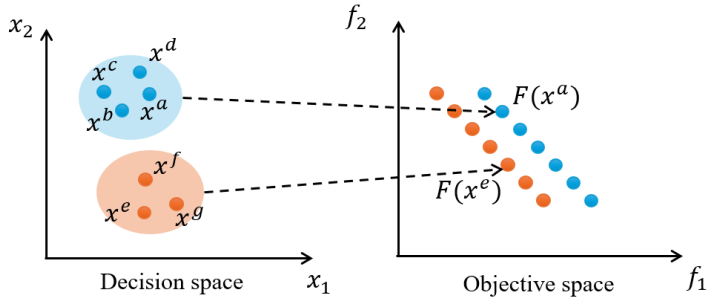



**Figure 2.** An example of MMOP with two objective functions, where $F(x^a) = F(x^b) = F(x^c) = F(x^d)$ and $F(x^e) = (Fx^f) = F(x^g)$.

For $x^i, x^j \in \Omega$, we say that $x^i$ *dominates* $x^j$, denoted as $x^i \succ x^j$, if and only if for all $f_\alpha \in f_1, \ldots, f_m$, $f_\alpha(x^i) \leq f_\alpha(x^j)$ and there exists some $f_\beta \in f_1, \ldots, f_m$ such that $f_\beta(x^i) < f_\beta(x^j)$. A solution $x \in \Omega$ is called a Pareto optimal solution, or non-dominated solution, if there does not exist any $x \succ x$. The set of all Pareto optimal solutions is called the Pareto set (PS), and the corresponding set of objective values is called the Pareto front (PF).

For an arbitrary solution $x^{L*} \in \Omega$, $x^{L*}$ is called a local Pareto optimal solution (LPS) if and only if there does not exist any $x \succ x^{L*}$ such that $|x - x^{L*}| \leq \theta$ (where $\theta$ is a small positive value) [26,27]. The local Pareto front (LPF) is the set of objective values corresponding to the LPS.

In the context of MOEAs, the global PS is typically considered to solve MOPs. However, for MMOPs, the PS refers to the global PS, while the LPS corresponds to the local optima. Without loss of generality, MMOPs can have multiple PSs, with at least one LPS. Note that the LPS does not include the global PS. The relationship between the LPS and the global PS is independent, and the size of the LPS is not necessarily related to the size of the global PS. In extreme cases, the size of the LPS can be as small as one.

### 2.2. Evolutionary Algorithm

Evolutionary algorithms (EAs) are heuristic algorithms [28] designed to solve optimization problems in an iterative manner. Inspired by the principles of natural evolution, EAs emulate the process of natural selection observed in living organisms.

Typically, EAs consist of five basic components, as shown in Figure 3. The algorithm begins by initializing a population of $N$ solutions. Next, parents are selected from the population, and offspring are generated through reproduction operators. The fitness of each solution is then calculated, with fitness serving as an indicator of the solution's quality. The mechanism for updating the population is called environmental selection, which compares the fitness of solutions and retains those with the highest quality. The algorithm iterates through the process of reproduction and environmental selection until a predefined termination criterion is satisfied.

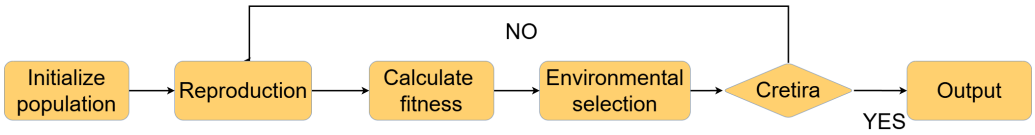



**Figure 3.** The framework of evolutionary algorithms.

In reproduction, tournament selection is used to select parents from the population and form a mating pool. The tournament selection process begins by randomly selecting two solutions from the population and comparing their fitness. The solution with the better fitness is added to the mating pool. This process is repeated until the mating pool is filled. Typically, the operators for reproducing offspring include crossover and mutation. For example, see Figure 4, in binary encoding, the crossover operator exchanges substrings before and after a specified locus between two strings. The mutation operator randomly flips some of the bits in the strings.

In the context of MMOPs, one key challenge is balancing the width and depth of exploration in the decision space. To address this, we use the GAhalf operator, which generates $N/2$ offspring in each generation. This operator aims to explore the decision space more thoroughly during the evolution process and generate a greater diversity of solutions.

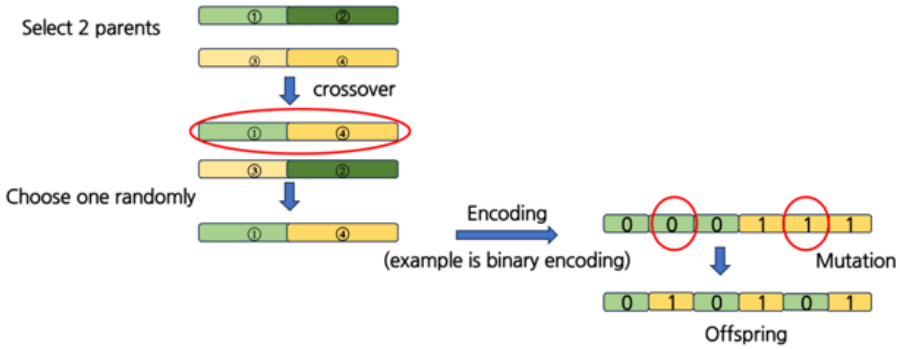



**Figure 4.** Crossover and a binary encoding example for mutation.

### *2.3. The Strategy for Evaluating Diversity*

In MMEA, improving environmental selection is effective in reducing the crowding of solutions, thereby increasing the diversity of the population. Among the numerous methods that enhance environmental selection, the Euclidean distance-based crowding distance calculates the crowding of a solution within a niche. This is defined as

$$CD(x^i) = \sum_{j=1}^{k_1} (k_1 - j + 1) d_{dec}(i, j) \tag{3}$$

where $CD(x^i)$ denotes the crowding distance of $x^i$, and $d_{dec}(i, j)$ denotes the Euclidean distance from the $x^i$ to the $k_1$ neighboring solutions. $k_1$ is a parameter that is suggested as 0.02 of the size of the population. In some cases, the crowding distance has limitations in balancing the diversity of solutions between the decision space and objective space due to the different scales of these spaces. Wang et al. [24] proposed the MO_Ring_CSO_SCD algorithm, which applies a special crowding distance (SCD) that considers both the decision space and the objective space. The SCD of a solution is defined as

$$SCD(x^i) = \begin{cases} \min(CD_{dec}(x^i), CD_{obj}(x^i)), & \text{if } CD_{dec}(x^i) > CD_{dec}^{avg} \text{ or } CD_{obj}(x^i) > CD_{obj}^{avg} \\ \max(CD_{dec}(x^i), CD_{obj}(x^i)), & \text{otherwise,} \end{cases}, \tag{4}$$

where $CD_{dec}(x^i)$ and $CD_{dec}(x^i)$ are the crowding distance of $x^i$ in the decision space and objective space, respectively. $CD_{dec}^{avg}$ and $CD_{obj}^{avg}$ are the average crowding distance in the decision space and objective space, respectively. By applying the SCD to calculate the crowding, the solutions in overcrowded regions will be given priority for removal. However, when SCD increases diversity, although it simultaneously enhances the exploration of the decision space and the objective space, it is possible that the population be updated by the solutions with poor convergence. Yue et al. [23] improved the SCD and proposed an improved crowding distance (ICD) to calculate the crowding of $x^i$ as

$$ICD(x^i) = \begin{cases} \min(CD_{dec}(x^i), \frac{CD_{obj}(x^i)}{PRank(x^i)}), & \text{if } CD_{dec}(x^i) > CD_{dec}^{avg} \text{ or } CD_{obj}(x^i) > CD_{obj}^{avg} \\ \max(CD_{dec}(x^i), CD_{obj}(x^i)), & \text{otherwise,} \end{cases}, \tag{5}$$

where $PRank(x^i)$ is the Pareto rank of $x^i$, which is expressed as

$$PRank(x^i) = 1 + |\{x^r | x^r \succ x^i, x^i \in P\}|. \tag{6}$$

The Pareto rank represents the number of solutions that dominate $x^i$ in the population. By integrating the Pareto rank, even if solutions have larger crowding distances, poor

convergence will lead them to be removed. Another important topic in MMEA is increasing the diversity of local optima. Some researchers have proposed strategies to identify local optima and prevent full convergence to global optima. Zhou et al. [29] proposed $P_{Q,\epsilon^-}MOEA$ that identifies a set of solutions with acceptable quality convergence by applying the $\epsilon$-dominance relationship. The $\epsilon$-dominance relationship saves all solutions in an unlimited achievement, and the LPSs can be located around the global PSs. Liu et al. [30] integrated the dual clustering method into the decision and objective space to find the local optima. Li et al. [25] proposed the Hierarchy Ranking method that applies the local convergence quality evaluation and dual clustering to preserve the local optima in the decision and objective space. The local convergence quality of a solution $x^i$ is defined as

$$LocalCon(x^i) = \frac{\sum_{j=1}^{n_i} B(x^i, x^j)}{n_i}, \tag{7}$$

$$B(x^i, x^j) = \begin{cases} 1, & x^i \succ x^j \\ 0, & \text{otherwise} \end{cases}, \tag{8}$$

where $n_i$ is the number of neighbors of solution $x^i$. Additionally, a user-defined parameter $\epsilon$ allows for flexible control over the quality of the LPF. Specifically, a solution $x^L$ is defined as an $\epsilon$-approximate solution if $F(x^L) \times (1-\epsilon)$ is not dominated by any other solutions in global PFs.

## 3. Proposed Methods

We propose the use of Gaussian similarity to reduce the crowding of solutions in both the decision space $\Omega$ and the objective space $R$. Based on this similarity, we introduce a new approach for assessing diversity fitness and a strategy for environmental selection. These methodologies are incorporated into MMEA, leading to the proposed MMEA-GS. In this section, we present Gaussian similarity in Section 3.1, provide an overview of the algorithm in Section 3.2, explain the calculation of diversity fitness in Section 3.3, describe the calculation of convergence fitness in Section 3.4, and outline the new environmental selection strategy in Section 3.5.

### *3.1. Gaussian Similarity*

In this chapter, we define Gaussian similarity and demonstrate that it reduces the crowding of solutions in neighboring regions by increasing the sensitivity of the closeness calculation between solution pairs. Specifically, Gaussian similarity evaluates the proximity between solutions in both the decision space and the objective space by transforming the distances between solution pairs into a high-dimensional space. The transformed values are then defined as Gaussian similarity. For two arbitrary solutions, $x^i$ and $x^j$, the Gaussian similarity $G(i,j)$ is defined as

$$G(i,j) = exp(-(\frac{d_{dec}^2(i,j)}{2\sigma_{dec}^2} + \frac{d_{obj}^2(i,j)}{2\sigma_{obj}^2})), \tag{9}$$

$$\sigma_{dec} = std(d_{dec}(i,j)), \quad \sigma_{obj} = std(d_{obj}(i,j)), \tag{10}$$

where $d_{obj}(i,j)$ and $d_{dec}(i,j)$ denote the Euclidean distance between solutions $x^i$ and $x^j$ in the objective space and decision space, respectively. $\sigma_{dec}$ and $\sigma_{obj}$ represent the standard deviation of the distances between solution pairs across the entire population in the decision space and objective space, respectively. Figure 5 illustrates the distribution of solution pairs in the population. It shows that as the distance between solutions $x^i$ and $x^j$ increases linearly,

$G(i,j)$, represented by point C in Figure 5, moves away from the peak of the surface. This implies that $G(i,j)$ decreases sharply. The Gaussian similarity is sensitive to the proximity of solution pairs. Once $d_{dec}(i,j)$ and $d_{obj}(i,j)$ change, the Gaussian similarity changes exponentially, and the corresponding solutions are prioritized for removal. By removing solutions with high Gaussian similarity, the crowding of solutions in a neighboring region is reduced, thereby improving the diversity of the population. At the same time, the values of $\sigma_{dec}$ and $\sigma_{obj}$ gradually decrease, causing the slope of the Gaussian surface to become gentler.

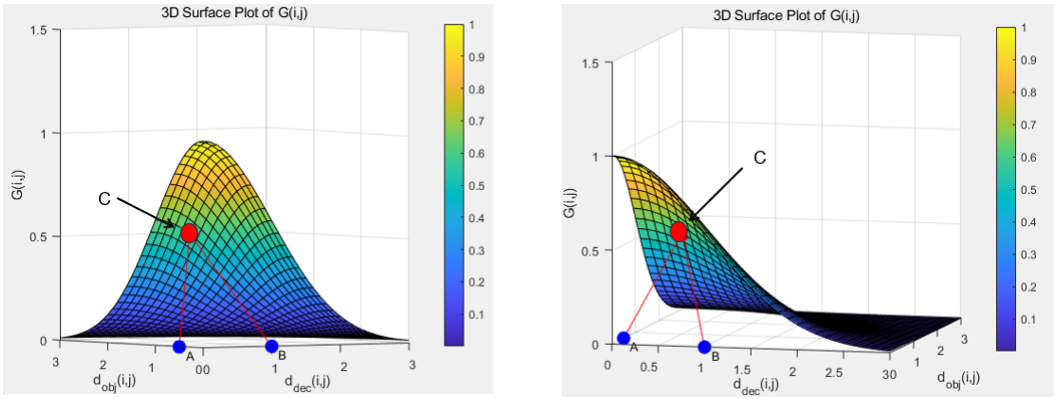



**Figure 5.** The surface is the distribution of Gaussian similarity of population. The left one is the side view of the surface and the right one is the front view of the surface. For $x^i$ and $x^j$, two blue points A and B represent $d_{obj}(i,j)$ and $d_{dec}(i,j)$, respectively. The point C represents the Gaussian similarity $G(i,j)$ between $x^i$ and $x^j$, which is computed by Equation (9).

### *3.2. Framework of MMEA-GS*

The MMEA-GS is described in Algorithm 1. Initially, the algorithm initializes the population $P$ of $N$ solutions. Then, for all solutions in P, the algorithm calculates the diversity fitness (DF) and convergence fitness (CF). While the number of fitness evaluation (FE) is less than the maximum number of FE (maxFE), the algorithm produces a mating pool by tournament selection and generates $N/2$ offspring $Q$ from the mating pool. Finally, the population $P$ is updated based on environmental selection.

**Algorithm 1** MMEA-GS

```
Initialize P with N solutions
Initialize DF and CF archive to P
while Not satisfy criteria do
    Form a Mating pool from P by selection
    Generate N/2 offspring Q from the Mating pool
    Calculate DF and CF for P and offspring
    Generate P_next from P ∪ Q by Environmental Selection
end while
```

### *3.3. Diversity Fitness*

We introduce a new strategy for calculating diversity fitness (DF) by integrating the Gaussian similarity. Algorithm 2 provides an overview of the DF calculation process.

**Algorithm 2** Computing Diversity Fitness

1: Scale the objective vector and decision variables to $[P_{dec}(x), P_{obj}(F(x))]$
2: Calculate the Euclidean distance of solutions in decision space and objective space
3: Calculate the niche radius ($nr$) of each solution in the population
4: Calculate $R(x^i)$ as the dominant relationship among solutions within the niche
5: Calculate $G(i, j)$ for each solution
6: Calculate the $GD(x^i)$
7: $DF = R_d(x^i) + GD(x^i)$

Initially, a solution $x$ is scaled to $P_{dec}(x)$ and objectives $F(x)$ is scaled to $P_{obj}(F(x))$ as follows:

$$P_{dec}(x) = \frac{x - x_{min}}{x_{max} - x_{min}}, \tag{11}$$

$$P_{obj}(F(x)) = \frac{F(x) - F_{min}(x)}{F_{max}(x) - F_{min}(x)}, \tag{12}$$

where $x_{min}$ and $x_{max}$ are the minimum and maximum variables in the decision space. $F_{max}(x)$ and $F_{min}(x)$ are the minimum and maximum objective vectors in objective space. We compute diversity dominant relationship $R_d(x^i)$ as follows:

$$\begin{aligned} R_d(x^i) &= \sum S(x^j) \\ s.t. \quad & x^j \succ x^i, d_{dec}(i, j) < nr, \end{aligned} \tag{13}$$

$$S_d(x^j) = |\{x^k \in P | x^j \succ x^k \text{ and } d_{dec}(j, k) < nr\}|, \tag{14}$$

where $nr$ is the niche radius of $x^i$ that calculates by the average distance to the nearest $n$ solutions. The $S_d(x^j)$ represents the quality of the solutions that dominate the solution $x^i$. The greater $S_d(x^j)$ is indicative of the $x^i$ that is at a disadvantage within a specific niche. The Gaussian Density (GD) of an arbitrary solution $x^i$ is defined as

$$GD(x^i) = \frac{\delta^k}{1 + 2\delta^k}, \tag{15}$$

$$\delta^k = max(d_{dec}(i, s), d_{obj}(i, s)), \tag{16}$$

where $\delta^k$ is calculated by the maximum distance of the decision space and objective space between $x^i$ and $x^s$. $x^s$ is a solution that has the highest Gaussian similarity among $k$ nearest solutions of $x^i$.

### *3.4. Convergence Fitness*

The convergence fitness is a metric to control the convergence speed and quality. We integrate the Gaussian density into the strategy of SPEA2 [12] to calculate convergence fitness. Algorithm 3 shows the procedure of convergence fitness calculation.

**Algorithm 3** Convergence Fitness

1: Scale the objective vector and decision variables to $[P_{dec}(x), P_{obj}(F(x))]$
2: Calculate the Euclidean distance of solutions in decision space and objective space
3: Calculate the niche radius ($nr$) of each solution in the population
4: Calculate $R_c(x^i)$ as the dominant relationship among solutions within the niche
5: Calculate $G(i, j)$ for each solution
6: Calculate the $GD(x^i)$
7: $CF = R_c(x^i) + GD(x^i)$

The scaling method for calculating the convergence fitness is the same as Equation (11) and Equation (12). Then, we compute the convergence dominant relationship $R_c(x^i)$, which is defined as

$$\begin{aligned} R_c(x^i) &= \sum S_c(x^j), \\ s.t. \quad x^i, x^i &\in P, x^i \succ x^i, \end{aligned} \tag{17}$$

$$S_c(x^j) = |\{x^k \in P | x^j \succ x^k\}|, \tag{18}$$

where $S_c(x^j)$ is a counter parameter to compute the number of solutions that is dominated by $x^j$. After that, the algorithm computes the Gaussian similarity and GD by Equation (9) and Equation (15), respectively.

### *3.5. Environmental Selection*

During the process of MMEA-GS, environmental selection emerges as the most significant mechanism for preserving the balance of diversity and convergence quality of the population. We introduce a mechanism of environmental selection based on Gaussian similarity that decreases the imbalance between diversity and convergence. Algorithm 4 provides an overview of the environmental selection of solutions.

**Algorithm 4** Environmental Selection

```
Calculate DF of Q
Compute the T as the number of solutions that DF < 1
if T < N then
    Sort the solutions of P ∪ Q by ascending order based on CF
    Update top N solutions to P
else
    Scale the decision vector and objective value to [P_dec(x), P_obj(F(x))]
    Calculate the Euclidean distance between each pair of solutions in Ω and R
    Calculate σ_dec, σ_obj, and τ
    Calculate G(i, j)
    Calculate BGD(i, j)
    Delete K solutions according to BGD
end if
```

We denote $Q$ as the set of all offspring, and $T = |\{DF(i) < 1 | i \in P \cup Q\}|$, which represents the number of solutions that have $DF < 1$. If $T$ is smaller than the population size $N$, it implies that there are not enough objective values of solutions reaching the PF. Thus, the algorithm continues to converge towards the PF as the primary goal. Otherwise, if there are enough solutions to reach the PF, the algorithm updates the population by replacing solutions with qualified ones. This replacement will be performed based on the balanced Gaussian distance (BGD). The BGD of a solution pair $x^i$ and $x^j$ is defined as

$$BGD(i,j) = \begin{cases} \min(d_{dec}(i,j), d_{obj}(i,j)) & G(i,j) > \tau \\ \max(d_{dec}(i,j), d_{obj}(i,j)) & otherwise \end{cases}, \tag{19}$$

where $\tau$ is the threshold. If the $G(i,j)$ surpasses the threshold, $x^i$ and $x^j$ are seen as over-proximate to each other. The Gaussian similarity between $x^i$ and $x^j$ considers the closeness in both the decision and objective space. When one of the spaces has a very small distance and the other has a large distance, $G(i,j)$ is not too small a value either. This time, the solutions are not preferentially deleted. Therefore, we propose a BGD that removes the worst solutions after filtering out the over-similar solutions by Gaussian similarity.

While environmental selection changes focus on increasing the diversity of the population, the environmental selection can be separated into two periods. In the first period, the algorithm improves the uniform distribution of the global PSs. However, when a part of the population is sufficiently well distributed on global PSs, i.e., the $BGD(i, j)$ of another part of the population is greater than $\tau$, then the global PSs will not be able to sustain more solutions. It will change to the second period, increasing the diversity for searching the LPSs. Since Equation (13) calculates the dominated relationship of solutions just in a niche, the solutions on global PSs and LPSs are seen as having the same convergence.

## 4. Experiments

### *4.1. Experiment Setting*

For the experiments, we use the IEEE CEC2019 MMF1-8 benchmarks [26], IDMP benchmarks [27], and IDMP_e benchmarks [25], encompassing a total of 28 problems. The selected benchmarks include three commonly used types—MMF, IDMP, and IDMP_e—that are widely adopted for evaluating the performance of multi-modal multi-objective evolutionary algorithms (MMEAs).

MMF benchmarks test the algorithm's ability to identify multiple global Pareto sets and evaluate convergence and diversity [26]. IDMP benchmarks introduce higher complexity by increasing the imbalance between convergence and diversity in the decision space, which is characterized by more discontinuous Pareto sets and larger distances between them [27]. IDMP_e benchmarks add the challenge of multiple local optima, testing the algorithm's capability to find both global and local Pareto sets [25]. Although these benchmarks do not directly represent real-world MMOPs, they capture key complexities observed in such problems, such as discontinuity, imbalance, and local optima. This enables a comprehensive evaluation of an algorithm's performance in balancing diversity between decision and objective spaces while maintaining convergence.

The MMF benchmarks are constructed by mirroring the original Pareto optimal solutions, creating multiple equivalent subsets, and are used to evaluate the capability to identify multiple global Pareto sets and assess performance in terms of convergence and diversity. IDMP benchmarks, with their increased complexity and imbalances, further test an algorithm's ability to manage diversity and convergence in challenging conditions. IDMP_e, a modified version of IDMP, includes multiple LPSs, making it suitable for testing the algorithm's ability to locate local optima. The true PFs, PSs, LPSs, and related parameters for each problem are based on [26,27].

Five state-of-the-art MMEA algorithms have been selected for comparison: DN-NSGA-II [19], MO_Ring_PSO-SCD [24], TriMOEA-TA&R [21], MMEA-WI [22], and HREA [25]. We used the parameters recommended in the respective papers for these algorithms, as shown in Table 1.

We set the maximum number of evaluations $maxFE$ as 40,000 and set the population size $N$ to 200, which was adopted by all algorithms. We set $\tau = 0.76$ for testing MMF1-8, and $\tau = 0.7$ for testing IDMP. All MMEAs were run 30 times independently on each benchmark problem. We introduced the Wilcoxon rank-sum test with $\alpha = 0.05$ to show the significant level of comparison. '+/−/=' refers to significantly better than MMEA-GS, worse than MMEA-GS, and similar to MMEA-GS, respectively. The values in brackets represent the standard deviations of the 30 runs.

**Table 1.** The related parameters of comparison algorithms.

| Algorithms | Setting |
|---|---|
| DN-NSGA-II | - |
| MO_Ring_PSO_SCD | $c_1 = c_2 = 2.05$, $\omega = 0.7298$, $n_{PBA} = 5$, $n_{NBA} = 15$ |
| TriMOEA-TA&R | $P_{com} = 0.5$, $\sigma_{nich} = 0.1$, $\epsilon_{peak} = 0.01$, $NR = 100$, $NCA = 20$, $NIA = 6$ |
| MMEA-WI | $\kappa = 0.05$ |
| HREA | $eps = 0.3$, $p = 0.5$ |

### *4.2. Performance Indicator*

This study mainly utilizes two indicators to evaluate the performance of the MMEA-GS, which are inverted generational distance (IGD) and inverted generational distance in decision space (IGDX) [31].

$$IGD(X) = \frac{1}{|X^*|} \sum_{y \in X^*} \min_{x \in X} \{d(F(x), F(y))\}, \tag{20}$$

$$IGDX(X) = \frac{1}{|X^*|} \sum_{y \in X^*} \min_{x \in X} \{d(x, y)\}, \tag{21}$$

where $X$ denotes the obtained final population. $X^*$ denotes the finite number of non-dominated solutions that are evenly distributed from the true PS. The $x$ refers to a solution in $X$, $y$ refers to a reference point in the true PSs. The lower IGD value indicates that the obtained population has better convergence and diversity in the objective space. Similar to the IGD, the lower IGDX value corresponds to the better performance of diversity and convergence in the decision space. By using both IGD and IGDX, we are able to assess both convergence and diversity across two spaces, which ensures that the algorithm maintains a balance between exploring the decision space and refining solutions that are already close to optimal. An MMEA is recognized as having good property if the population has a satisfied IGDX and an acceptable IGD, while the IGD and IGDX are in conflict.

### *4.3. Comparison Results*

Table 2 presents the IGD comparison results of five state-of-the-art MMEA algorithms across 20 typical MMOPs. The results clearly demonstrate that MMEA-GS outperforms the other MMEAs. Specifically, MMEA-GS achieves the lowest IGD values on 14 test problems, showcasing its strong capability in balancing convergence and diversity within the objective space. In contrast, HREA obtained the best IGD values on five test problems, particularly in the IDMPM4T1-4 test suite. This is because IDMPM4T1-4 involves four objective functions and decision space dimensions, and HREA utilizes a local convergence indicator that searches smaller neighboring regions for each solution. This approach is particularly effective for problems with four dimensions. However, this focus on local convergence can limit overall population convergence when applied to smaller regions. For the remaining MMEAs, MMEA-GS consistently shows significant improvements.

The IGDX comparison results are presented in Table 3. MMEA-GS achieves the best results on 10 problems and the second-best on eight problems. Additionally, the Wilcoxon rank-sum test comparison further confirms MMEA-GS's superior performance in solving MMOPs. HREA achieved the best IGDX values on seven problems and second-best on nine, but its reliance on the local convergence indicator remains a limitation. While this indicator improves convergence in smaller regions, it compromises diversity in the decision space, as it excessively focuses on local convergence. In conclusion, MMEA-GS demonstrates

substantial superiority over other algorithms, significantly enhancing the balance between convergence and diversity in both the decision and objective spaces.

**Table 2.** Comparison for IGD values of IDMP and MMF.

| Problem | DN-NSGA-II | B_Ring_PSO_SCD | TriMOEA-TA&R | MMEAWI | HREA | MMEA-GS |
|---|---|---|---|---|---|---|
| IDMPM2T1 | 5.0240e-4 (1.77e-5) − | 1.1363e-3 (6.43e-5) − | 6.7193e-4 (3.17e-5) − | 6.3792e-4 (2.51e-5) − | 4.8440e-4 (1.59e-5) − | **4.7517e-4 (1.15e-5)** |
| IDMPM2T2 | 5.0609e-4 (2.91e-5) − | 7.0539e-4 (3.15e-5) − | 6.8493e-4 (3.68e-5) − | 6.4952e-4 (3.05e-5) − | 5.0787e-4 (1.25e-5) − | **4.8695e-4 (1.24e-5)** |
| IDMPM2T3 | 4.9396e-4 (4.89e-5) = | 6.9926e-4 (2.36e-5) − | 1.4163e-2 (2.91e-2) − | 6.7290e-4 (3.75e-5) − | 5.5539e-4 (1.73e-5) − | **4.9001e-4 (1.83e-5)** |
| IDMPM2T4 | 4.9490e-4 (2.00e-5) = | 7.0747e-4 (3.65e-5) − | 7.0067e-4 (2.53e-5) − | 6.9146e-4 (4.12e-5) − | 4.7639e-4 (1.46e-5) = | **4.7567e-4 (1.28e-5)** |
| IDMPM3T1 | 6.3731e-3 (1.89e-4) − | 8.1965e-3 (3.61e-4) − | 1.1594e-2 (9.87e-4) − | 6.0868e-3 (1.50e-4) − | 5.6571e-3 (1.17e-4) − | **5.5957e-3 (1.07e-4)** |
| IDMPM3T2 | 6.3884e-3 (2.38e-4) − | 6.7507e-3 (1.93e-4) − | 1.1623e-2 (9.07e-4) − | 6.1092e-3 (2.29e-4) − | 5.6103e-3 (1.23e-4) = | **5.5415e-3 (1.08e-4)** |
| IDMPM3T3 | 6.3673e-3 (2.06e-4) − | 6.8035e-3 (2.30e-4) − | 1.1312e-2 (9.78e-4) − | 6.3241e-3 (1.67e-4) − | 5.6967e-3 (1.40e-4) = | **5.6469e-3 (1.43e-4)** |
| IDMPM3T4 | 6.2748e-3 (1.81e-4) − | 6.7555e-3 (2.55e-4) − | 1.1882e-2 (6.43e-4) − | 6.0116e-3 (2.27e-4) − | 5.5637e-3 (9.83e-5) − | **5.4572e-3 (1.22e-4)** |
| IDMPM4T1 | 9.3446e-3 (3.16e-4) − | 1.9968e-2 (1.08e-3) − | 2.6985e-2 (1.71e-3) − | 8.8506e-3 (3.46e-4) − | **7.9390e-3 (7.46e-4) +** | 8.4503e-3 (3.20e-4) |
| IDMPM4T2 | 8.5886e-3 (2.80e-4) − | 1.2847e-2 (7.55e-4) − | 2.6582e-2 (1.73e-3) − | 8.4047e-3 (3.79e-4) − | **7.6094e-3 (5.65e-4) +** | 7.9856e-3 (2.65e-4) |
| IDMPM4T3 | 8.7228e-3 (3.67e-4) − | 1.2867e-2 (8.06e-4) − | 3.0646e-2 (1.42e-2) − | 8.9597e-3 (2.46e-4) − | **7.3029e-3 (5.37e-4) +** | 8.0933e-3 (2.19e-4) |
| IDMPM4T4 | 8.5091e-3 (1.84e-4) − | 1.3478e-2 (8.79e-4) − | 2.6418e-2 (1.49e-3) − | 8.5887e-3 (3.51e-4) − | **7.4775e-3 (5.82e-4) +** | 7.7849e-3 (3.08e-4) |
| MMF1 | 3.1410e-3 (1.27e-4) − | 4.2560e-3 (3.83e-4) − | 3.5791e-3 (9.21e-4) − | 3.7216e-3 (2.81e-4) − | 3.8353e-3 (2.28e-4) − | **2.3655e-3 (5.35e-5)** |
| MMF2 | 5.2009e-3 (2.51e-3) − | 2.6584e-2 (1.22e-2) − | 1.3927e-2 (1.65e-2) − | 4.4808e-3 (3.49e-4) = | 4.7638e-3 (2.19e-3) = | **4.4383e-3 (8.50e-4)** |
| MMF3 | 4.4534e-3 (2.83e-3) = | 1.8329e-2 (4.98e-3) − | 9.9811e-3 (9.23e-3) − | 4.0996e-3 (2.78e-4) − | **3.8587e-3 (7.55e-4) =** | 3.8887e-3 (5.92e-4) |
| MMF4 | 3.1144e-3 (1.20e-4) − | 3.4337e-3 (1.87e-4) − | 3.5197e-2 (7.26e-2) − | 3.7135e-3 (2.26e-4) − | 3.3886e-3 (1.12e-4) − | **3.0179e-3 (9.62e-5)** |
| MMF5 | 3.1537e-3 (1.48e-4) − | 3.5657e-3 (1.72e-4) − | 3.4206e-3 (1.47e-3) − | 3.5874e-3 (2.84e-4) − | 3.8979e-3 (2.34e-4) − | **2.8915e-3 (1.27e-4)** |
| MMF6 | 3.1328e-3 (1.05e-4) − | 3.6095e-3 (2.42e-4) − | 3.1424e-3 (7.38e-5) − | 3.5155e-3 (2.43e-4) − | 4.0536e-3 (2.55e-4) − | **2.8739e-3 (9.53e-5)** |
| MMF7 | 3.5339e-3 (2.21e-4) − | 3.5166e-3 (2.09e-4) − | 3.9440e-3 (1.51e-3) − | 4.0177e-3 (2.56e-4) − | 3.9317e-3 (2.63e-4) − | **2.4097e-3 (4.86e-5)** |
| MMF8 | 3.9491e-3 (3.63e-4) − | **3.5153e-3 (1.93e-4) =** | 4.5947e-3 (4.64e-3) − | 3.5987e-3 (2.21e-4) = | 3.6656e-3 (2.65e-4) = | 3.5382e-3 (1.92e-4) |
| +/−/= | 0/18/2 | 0/19/1 | 0/20/0 | 0/18/2 | 4/10/6 | |

**Table 3.** Comparison for IGDX values of IDMP and MMF.

| Problem | DN-NSGA-II | MO_Ring_PSO_SCD | TriMOEA-TA&R | MMEAWI | HREA | MMEA-GS |
|---|---|---|---|---|---|---|
| IDMPM2T1 | 6.0594e-1 (2.05e-1) − | 8.3653e-2 (2.00e-1) − | 5.8359e-1 (2.33e-1) − | 8.1440e-4 (3.87e-5) − | **5.3005e-4 (1.17e-5) +** | 5.4236e-4 (2.68e-5) |
| IDMPM2T2 | 3.5942e-1 (3.41e-1) − | 2.5874e-3 (1.09e-3) − | 5.6157e-1 (2.54e-1) − | 1.0035e-3 (4.43e-5) − | 8.0810e-4 (3.39e-5) − | **6.4021e-4 (6.24e-5)** |
| IDMPM2T3 | 1.4711e-1 (2.68e-1) − | 1.9519e-3 (2.91e-4) − | 2.2267e-1 (3.01e-1) − | 1.3419e-3 (8.36e-5) − | 1.1367e-3 (5.32e-5) − | **1.0903e-3 (2.91e-4)** |
| IDMPM2T4 | 6.0595e-1 (2.05e-1) − | 2.4695e-2 (1.23e-1) − | 6.5085e-1 (1.23e-1) − | 9.2164e-4 (6.36e-5) − | **5.2969e-4 (9.88e-6) +** | 5.4485e-4 (2.49e-5) |
| IDMPM3T1 | 6.6041e-1 (3.36e-1) − | 1.1621e-1 (1.72e-1) − | 7.3857e-1 (2.98e-1) − | 9.4122e-3 (1.69e-4) − | 8.1604e-3 (1.07e-4) = | **8.1253e-3 (2.01e-4)** |
| IDMPM3T2 | 5.4811e-1 (2.69e-1) − | 4.3511e-2 (7.46e-2) − | 6.4903e-1 (2.52e-1) − | 9.5927e-3 (3.33e-4) − | **8.1109e-3 (1.20e-4) =** | 8.1539e-3 (1.20e-4) |
| IDMPM3T3 | 3.5599e-1 (2.37e-1) − | 1.3148e-2 (9.09e-4) − | 4.9577e-1 (3.33e-1) − | 1.0072e-2 (2.89e-4) − | 8.6470e-3 (1.52e-4) = | **8.6467e-3 (1.52e-4)** |
| IDMPM3T4 | 8.2283e-1 (2.28e-1) − | 5.0254e-2 (8.46e-2) − | 7.7390e-1 (2.29e-1) − | 1.5237e-1 (1.65e-1) − | **8.0044e-3 (9.37e-5) =** | 3.2504e-2 (7.46e-2) |
| IDMPM4T1 | 1.1695e+0 (8.71e-2) − | 7.7589e-1 (3.62e-1) − | 1.1382e+0 (2.26e-1) − | 1.0787e-1 (1.29e-1) − | 2.0463e-1 (1.98e-1) − | **1.8707e-2 (4.78e-2)** |
| IDMPM4T2 | 1.1010e+0 (1.69e-1) − | 1.6445e-1 (1.97e-1) − | 1.0984e+0 (1.39e-1) − | 3.7747e-1 (3.49e-1) − | 2.0328e-1 (1.62e-1) − | **3.6200e-2 (8.04e-2)** |
| IDMPM4T3 | 9.2329e-1 (2.48e-1) − | **1.7634e-2 (1.06e-3) +** | 9.5905e-1 (2.44e-1) − | 2.1294e-1 (2.04e-1) − | 3.6677e-1 (3.04e-1) − | 4.6834e-2 (8.94e-2) |
| IDMPM4T4 | 1.0530e+0 (2.30e-1) − | **5.1726e-2 (7.75e-2) =** | 1.0422e+0 (2.04e-1) − | 3.8948e-1 (1.68e-1) − | 3.6666e-1 (2.65e-1) − | 1.5819e-1 (1.32e-1) |
| MMF1 | 4.1110e-2 (9.69e-4) − | 6.7275e-2 (1.21e-2) − | 5.0714e-2 (5.05e-3) − | 3.9193e-2 (1.91e-3) − | **3.2002e-2 (7.13e-4) +** | 3.4079e-2 (6.23e-4) |
| MMF2 | 3.2780e-2 (1.70e-2) − | 5.5881e-2 (2.57e-2) − | 4.8629e-2 (2.81e-2) − | 1.2867e-2 (5.80e-3) − | 1.0914e-2 (3.34e-3) = | **1.0343e-2 (2.97e-3)** |
| MMF3 | 2.5762e-2 (1.83e-2) − | 4.3399e-2 (1.99e-2) − | 3.8107e-2 (3.12e-2) − | 9.7669e-3 (1.68e-3) − | 8.9076e-3 (2.26e-3) = | **8.5645e-3 (1.07e-3)** |
| MMF4 | 2.6839e-2 (1.87e-3) − | 5.6971e-2 (1.50e-2) − | 9.3048e-2 (1.48e-1) − | 2.3443e-2 (6.59e-4) − | **1.8142e-2 (5.44e-4) +** | 1.8495e-2 (7.01e-4) |
| MMF5 | 8.0618e-2 (4.85e-3) − | 1.1825e-1 (1.46e-2) − | 8.5819e-2 (8.32e-3) − | 6.8953e-2 (2.69e-3) − | 5.7274e-2 (2.01e-3) = | **5.7091e-2 (8.54e-4)** |
| MMF6 | 7.0379e-2 (3.28e-3) − | 1.0179e-1 (1.10e-2) − | 7.6473e-2 (6.21e-3) − | 6.1668e-2 (2.48e-3) − | 5.3907e-2 (1.21e-3) − | **5.2662e-2 (6.30e-4)** |
| MMF7 | 2.2156e-2 (1.05e-3) − | 4.9354e-2 (1.36e-2) − | 3.2532e-2 (2.27e-2) − | 2.3855e-2 (1.15e-3) − | 1.9323e-2 (8.39e-4) − | **1.7330e-2 (5.33e-4)** |
| MMF8 | 6.8334e-2 (1.61e-2) − | 1.7083e-1 (6.92e-2) − | 4.5395e-1 (9.22e-2) − | 4.9998e-2 (4.34e-3) − | **3.6433e-2 (1.30e-3) =** | 3.7568e-2 (2.39e-3) |
| +/−/= | 0/20/0 | 1/18/1 | 0/20/0 | 0/20/0 | 4/8/8 | |

### *4.4. Performance in Identifying LPSs*

A series of experiments were conducted to assess the ability of MMEA-GS to identify LPSs, an important aspect of solving multi-modal optimization problems (MMOPs). The IDMP_e benchmark problems, which contain multiple local optima, were used for testing. Tables 4 and 5 present the results for the IGD and IGDX values, respectively. It is evident that MMEA-GS outperforms DN-NSGA-II, TriMOEA-TA&R, and MMEA-WI in identifying and optimizing LPSs.

Notably, MO_Ring_PSO_SCD achieved the best IGD values in three cases, surpassing other MMEAs on the problems IDMPM2T_1_e, IDMPM3T_2_e, and IDMPM3T_4_e. MO_Ring_PSO_SCD does not specifically address the challenge of identifying LPSs, which are critical for ensuring comprehensive optimization in MMOPs. While it effectively identi-

fies global Pareto solutions, it does not differentiate between global and local Pareto sets, limiting its performance in problems with multiple optima. In contrast, MMEA-GS is explicitly designed to address the challenge of balancing convergence and diversity when identifying both global and local Pareto solutions. MMEA-GS incorporates a diversity fitness criterion that enables it to maintain and explore LPSs. Unlike the MO_Ring_PSO_SCD, which treats convergence equally for global solutions only, MMEA-GS calculates convergence for local Pareto optimal solutions in the same manner as for global Pareto optimal solutions, ensuring that both types of solutions are effectively preserved and explored. This enhanced capability allows MMEA-GS to maintain a more balanced population of solutions, which contributes to its superior performance in IGDX, particularly in preserving diversity in the decision space.

While HREA benefits from a local convergence indicator, it still lags behind MMEA-GS in both the decision space and the objective space, especially when considering the identification of multiple local optima. These results highlight the advantage of MMEA-GS in addressing the local optima problem by maintaining a better balance between convergence and diversity, making it more suitable for problems that require the identification of multiple local optima.

**Table 4.** Comparison for IGD values of IDMP_e.

| Problem | DN-NSGA-II | MO_Ring_PSO_SCD | TriMOEA-TA&R | MMEA-WI | HREA | MMEA-GS |
|---|---|---|---|---|---|---|
| IDMPM2T1_e | 7.2418e-3 (1.44e-5) + | **6.9602e-3 (4.98e-5) +** | 7.4226e-3 (3.81e-6) − | 7.2717e-3 (3.13e-5) + | 7.4109e-3 (2.51e-5) = | 7.4119e-3 (2.78e-5) |
| IDMPM2T2_e | 7.2646e-3 (1.78e-5) − | 7.1750e-3 (3.36e-5) − | 7.4315e-3 (3.68e-6) − | 7.2826e-3 (2.75e-5) − | **8.3520e-4 (2.39e-5) +** | 9.3897e-4 (2.14e-5) |
| IDMPM2T3_e | 5.0016e-3 (1.18e-5) − | 5.6398e-3 (4.63e-4) − | 2.2192e-2 (2.92e-2) − | 5.1500e-3 (2.68e-5) − | 9.3207e-4 (2.86e-5) − | **8.0296e-4 (1.21e-5)** |
| IDMPM2T4_e | 1.6576e-2 (3.00e-3) = | 1.5489e-2 (1.11e-4) + | 1.5298e-2 (2.99e-3) + | 1.6229e-2 (2.78e-5) = | 1.6490e-2 (6.31e-5) − | **1.6059e-2 (1.85e-3)** |
| IDMPM3T1_e | 2.5882e-2 (2.33e-4) − | 2.4139e-2 (2.75e-4) − | 2.9380e-2 (4.58e-4) − | 2.5715e-2 (1.23e-4) − | **7.6221e-3 (2.59e-4) +** | 9.6425e-3 (2.51e-4) |
| IDMPM3T2_e | 3.7879e-2 (2.73e-4) = | **3.6387e-2 (3.13e-4) =** | 4.2300e-2 (4.75e-3) − | 3.7323e-2 (1.89e-4) = | 3.8031e-2 (2.68e-4) = | 3.7841e-2 (3.75e-4) |
| IDMPM3T3_e | 3.7915e-2 (2.46e-4) − | 3.6713e-2 (3.16e-4) − | 4.1336e-2 (4.51e-4) − | 3.6947e-2 (2.83e-4) − | 1.7635e-2 (2.19e-4) − | **1.5914e-2 (3.43e-4)** |
| IDMPM3T4_e | 4.7019e-2 (3.20e-4) − | **3.6586e-2 (7.76e-4) +** | 4.2846e-2 (6.56e-3) − | 3.7302e-2 (2.23e-4) = | 3.8017e-2 (3.33e-4) = | 3.7076e-2 (5.76e-4) |
| +/−/= | 1/5/2 | 3/4/1 | 1/7/0 | 1/4/3 | 2/3/3 | |

**Table 5.** Comparison for IGDX values of IDMP_e.

| Problem | DN-NSGA-II | MO_Ring_PSO_SCD | TriMOEATAR | MMEAWI | HREA | MMEA-GS |
|---|---|---|---|---|---|---|
| IDMPM2T1_e | 6.7320e-1 (1.74e-5) − | 6.7348e-1 (2.97e-4) − | 6.7327e-1 (7.62e-6) − | 6.7330e-1 (2.21e-4) − | 6.2242e-1 (7.41e-5) − | **5.2983e-4 (8.28e-6)** |
| IDMPM2T2_e | 6.7334e-1 (7.26e-5) − | 6.7341e-1 (3.52e-4) − | 6.7327e-1 (9.56e-6) − | 6.7340e-1 (2.13e-4) − | 9.2091e-4 (4.09e-5) − | **6.9131e-4 (5.25e-5)** |
| IDMPM2T3_e | 5.0460e-1 (1.74e-1) − | 2.9840e-1 (9.51e-2) + | 5.4163e-1 (1.52e-1) − | 3.0097e-1 (4.07e-4) − | **1.1141e-3 (2.27e-5)** + | 3.0048e-1 (6.57e-5) |
| IDMPM2T4_e | 1.0184e+0 (3.16e-2) − | 1.0079e+0 (4.62e-4) − | 1.0125e+0 (2.77e-2) − | 1.0081e+0 (2.94e-4) − | **2.1936e-3 (1.23e-4) +** | 2.4356e-1 (6.80e-2) |
| IDMPM3T1_e | 7.0000e-1 (1.51e-1) − | 6.3565e-1 (8.27e-3) − | 8.1608e-1 (1.81e-1) − | 6.2535e-1 (7.96e-4) − | **8.4579e-3 (1.23e-4) +** | 8.6215e-3 (1.28e-4) |
| IDMPM3T2_e | 8.2657e-1 (1.52e-1) − | 5.1275e-1 (7.02e-2) − | 8.5937e-1 (1.25e-1) − | 4.9684e-1 (1.04e-3) − | 2.5547e-1 (8.29e-4) − | **8.7279e-3 (1.44e-4)** |
| IDMPM3T3_e | 7.2474e-1 (2.60e-1) − | 5.0038e-1 (2.03e-3) − | 8.3393e-1 (2.46e-1) − | 4.9862e-1 (1.09e-3) − | 2.5422e-1 (1.36e-3) − | **9.3147e-3 (1.33e-4)** |
| IDMPM3T4_e | 1.0035e+0 (1.46e-1) − | 8.5156e-1 (6.77e-3) − | 9.8068e-1 (1.66e-1) − | 9.1004e-1 (1.40e-1) − | 5.0367e-1 (5.97e-4) − | **3.8179e-1 (1.07e-1)** |
| +/−/= | 0/8/0 | 1/7/0 | 0/8/0 | 0/8/0 | 3/5/0 | |

### *4.5. Discussion*

The results demonstrate that Gaussian similarity effectively balances diversity between the decision and objective spaces while maintaining convergence. By comprehensively evaluating the closeness between solutions in both spaces, Gaussian similarity enables the environmental selection process to update populations with consideration for both dimensions. In contrast, SCD and ICD calculate crowding separately in the decision and objective spaces. This separate evaluation can lead to bias, as the space with a smaller scale is more likely to be deemed overcrowded, resulting in an imbalance in diversity maintenance between the two spaces.

However, our study reveals a limitation in MMEA-GS related to its sensitivity to the parameter $\tau$, which is currently chosen empirically based on extensive experimentation. While this approach performs well in many scenarios, it lacks adaptability for MMOPs with varying dimensions and complexities. As problem complexity and dimensionality

increase, the decision space's structure changes, causing the Gaussian distribution's surface to become steeper. This shift makes a constant $\tau$ classify a larger proportion of solutions as overcrowded, diminishing the algorithm's ability to maintain diversity and increasing computational time.

This phenomenon, also observed in related methods when computing crowding distances, highlights the need for an adaptive approach. To address this limitation, we propose designing $\tau$ as a dynamic parameter that adjusts throughout the optimization process. By enabling $\tau$ to adapt to the characteristics of different problem instances, MMEA-GS could better handle diverse challenges, improving scalability and robustness. This enhancement would lead to more efficient performance across a broader range of MMOPs, ensuring both convergence and diversity are maintained effectively.

## 5. Conclusions

In this paper, we propose Gaussian similarity, BGD, and MMEA-GS, a novel framework for solving MMOPs. Gaussian similarity is the first indicator to simultaneously evaluate crowding in both the decision and objective spaces, effectively enhancing diversity across both spaces. BGD ensures balanced diversity by preventing bias towards either space, enabling MMEA-GS to maintain convergence while promoting diversity. The experimental results demonstrate that MMEA-GS significantly improves both convergence and diversity compared to state-of-the-art algorithms. Notably, MMEA-GS achieved the lowest IGD values on MMF and IDMP problems and excelled in identifying LPSs in IDMP_e problems.

We conducted a comprehensive performance comparison using the Wilcoxon rank-sum test, which revealed statistically significant differences favoring MMEA-GS over benchmark algorithms (DN-NSGA-II, MO_Ring_PSO_SCD, TriMOEATAR, and MMEA-WI) in terms of balancing convergence and diversity, particularly on MMF and IDMP problems. This demonstrates MMEA-GS's effectiveness in addressing the imbalance between convergence and diversity for problems with multiple Pareto sets. Furthermore, MMEA-GS outperformed existing methods on IDMP_e problems by effectively maintaining diversity in LPSs while ensuring convergence. While other algorithms, such as DN-NSGA-II and MO_Ring_PSO_SCD, failed to balance these aspects, MMEA-GS consistently excelled. Although HREA identified LPSs using a local convergence indicator, it lagged behind MMEA-GS in maintaining diversity and convergence simultaneously.

The primary challenge in these evaluations was ensuring that diversity was preserved in both objective and decision spaces while converging to the correct PSs. Traditional approaches, which worked well for single global PSs, struggled in handling problems with multiple widely spaced PSs or identifying local solutions in more complex settings. MMEA-GS effectively addressed these challenges, offering a robust solution to MMOPs.

Future work will focus on refining the BGD mechanism for environmental selection by introducing adaptive techniques that dynamically adjust parameters during the optimization process. This will further enhance the algorithm's ability to balance diversity and convergence across diverse problem landscapes, improving its scalability and robustness for high-dimensional and complex MMOPs.

**Author Contributions:** Conceptualization, S.W. and D.-J.C.; methodology, S.W. and D.-J.C.; validation, D.-J.C.; formal analysis, S.W. and D.-J.C.; investigation, S.W. and D.-J.C.; writing—original draft preparation, S.W.; writing—review and editing, D.-J.C.; supervision, D.-J.C.; project administration, D.-J.C.; funding acquisition, D.-J.C. All authors have read and agreed to the published version of the manuscript.

**Funding:** This work was supported by the Institute of Information & Communications Technology Planning & Evaluation (IITP) under the Artificial Intelligence Convergence Innovation Human

Resources Development (IITP-2024-RS-2023-00255968) grant and the National Research Foundation of Korea (NRF-2022R1G1A1013287).

**Data Availability Statement:** The original contributions presented in this study are included in the article. Further inquiries can be directed to the corresponding author.

**Conflicts of Interest:** The authors declare no conflicts of interest.

## Abbreviations

The following abbreviations are used in this paper:

| | |
|---|---|
| MOPs | Multi-objective optimization problems |
| MMOPs | Multi-modal multi-objective optimization problems |
| MOEA | Multi-objective optimization evolutionary algorithm |
| MMEA | Multi-modal multi-objective evolutionary algorithm |
| MMEA-GS | Multi-Modal Multi-Objective Evolutionary Algorithm based on Gaussian Similarity |
| PS | Pareto set |
| PF | Pareto Front |
| LPS | Local Pareto set |
| LPF | Local Pareto front |
| SPEA | Strength Pareto evolutionary algorithm |
| SCD | Special crowding distance |
| ICD | Improved crowding distance |
| BGD | Balanced Gaussian similarity |

## References

1. Mayer, M.J.; Szilágyi, A.; Gróf, G. Environmental and economic multi-objective optimization of a household level hybrid renewable energy system by genetic algorithm. *Appl. Energy* **2020**, *269*, 115058. [CrossRef]
2. Huang, G.; Loucks, D.P. An inexact two-stage stochastic programming model for water resources management under uncertainty. *Civ. Eng. Syst.* **2000**, *17*, 95–118. [CrossRef]
3. Rao, S.S. *Engineering Optimization: Theory and Practice*; John Wiley & Sons: Hoboken, NJ, USA, 2019.
4. Craft, D.L.; Halabi, T.F.; Shih, H.A.; Bortfeld, T.R. Approximating convex Pareto surfaces in multiobjective radiotherapy planning. *Med. Phys.* **2006**, *33*, 3399–3407. [CrossRef]
5. Deb, K.; Sindhya, K.; Hakanen, J. Multi-objective optimization. In *Decision Sciences*; CRC Press: Boca Raton, FL, USA, 2016; pp. 161–200.
6. Tian, Y.; Si, L.; Zhang, X.; Cheng, R.; He, C.; Tan, K.C.; Jin, Y. Evolutionary large-scale multi-objective optimization: A survey. *ACM Comput. Surv. (CSUR)* **2021**, *54*, 1–34. [CrossRef]
7. Ehrgott, M.; Ide, J.; Schöbel, A. Minmax robustness for multi-objective optimization problems. *Eur. J. Oper. Res.* **2014**, *239*, 17–31. [CrossRef]
8. Deshmukh, S.; Agarwal, M.; Gupta, S.; Kumar, N. MOEA for discovering Pareto-optimal process models: An experimental comparison. *Int. J. Comput. Sci. Eng.* **2020**, *21*, 446–456. [CrossRef]
9. Li, K.; Wang, R.; Zhang, T.; Ishibuchi, H. Evolutionary Many-Objective Optimization: A Comparative Study of the State-of-the-Art. *IEEE Access* **2018**, *6*, 26194–26214. [CrossRef]
10. Pereira, J.L.J.; Oliver, G.A.; Francisco, M.B.; Cunha Jr, S.S.; Gomes, G.F. A review of multi-objective optimization: Methods and algorithms in mechanical engineering problems. *Arch. Comput. Methods Eng.* **2022**, *29*, 2285–2308. [CrossRef]
11. Yan, X.; Zhao, W. A novel select-best and prepotency evolution algorithm and its application to develop industrial oxidation reaction macrokinetic model. *Comput. Chem. Eng.* **2006**, *30*, 807–815. [CrossRef]
12. Liu, X.; Zhang, D. Multi-objective Investment Decision Making Based on an Improved SPEA2 Algorithm. In Proceedings of the Artificial Intelligence and Security: 5th International Conference, ICAIS 2019, New York, NY, USA, 26–28 July 2019; Proceedings, Part I 5; Springer: Berlin/Heidelberg, Germany, 2019; pp. 434–443.
13. Gadhvi, B.; Savsani, V.; Patel, V. Multi-objective optimization of vehicle passive suspension system using NSGA-II, SPEA2 and PESA-II. *Procedia Technol.* **2016**, *23*, 361–368. [CrossRef]
14. Deb, K.; Pratap, A.; Agarwal, S.; Meyarivan, T. A fast and elitist multiobjective genetic algorithm: NSGA-II. *IEEE Trans. Evol. Comput.* **2002**, *6*, 182–197. [CrossRef]

15. Gao, X.; He, F.; Zhang, S.; Luo, J.; Fan, B. A fast nondominated sorting-based MOEA with convergence and diversity adjusted adaptively. *J. Supercomput.* **2024**, *80*, 1426–1463. [CrossRef]
16. Ochoa, G.; Chicano, F. Local optima network analysis for MAX-SAT. In Proceedings of the Genetic and Evolutionary Computation Conference Companion, New York, NY, USA, 13–17 July 2019; GECCO '19; pp. 1430–1437. [CrossRef]
17. Selim, S.Z.; Ismail, M.A. K-Means-Type Algorithms: A Generalized Convergence Theorem and Characterization of Local Optimality. *IEEE Trans. Pattern Anal. Mach. Intell.* **1984**, *PAMI-6*, 81–87. [CrossRef] [PubMed]
18. Yue, C.; Qu, B.; Yu, K.; Liang, J.; Li, X. A novel scalable test problem suite for multimodal multiobjective optimization. *Swarm Evol. Comput.* **2019**, *48*, 62–71. [CrossRef]
19. Liang, J.J.; Yue, C.T.; Qu, B.Y. Multimodal multi-objective optimization: A preliminary study. In Proceedings of the 2016 IEEE Congress on Evolutionary Computation (CEC), Vancouver, BC, Canada, 24–29 July 2016; pp. 2454–2461. [CrossRef]
20. Liu, Y.; Ishibuchi, H.; Nojima, Y.; Masuyama, N.; Shang, K. A Double-Niched Evolutionary Algorithm and Its Behavior on Polygon-Based Problems. In Proceedings of the Parallel Problem Solving from Nature, Coimbra, Portugal, 8–12 September 2018.
21. Liu, Y.; Yen, G.G.; Gong, D. A Multimodal Multiobjective Evolutionary Algorithm Using Two-Archive and Recombination Strategies. *IEEE Trans. Evol. Comput.* **2019**, *23*, 660–674. [CrossRef]
22. Li, W.; Zhang, T.; Wang, R.; Ishibuchi, H. Weighted Indicator-Based Evolutionary Algorithm for Multimodal Multiobjective Optimization. *IEEE Trans. Evol. Comput.* **2021**, *25*, 1064–1078. [CrossRef]
23. Yue, C.; Suganthan, P.; Liang, J.; Qu, B.; Yu, K.; Zhu, Y.; Yan, L. Differential evolution using improved crowding distance for multimodal multiobjective optimization. *Swarm Evol. Comput.* **2021**, *62*, 100849. [CrossRef]
24. Wang, Y.; Yang, Z.; Guo, Y.; Zhu, J.; Zhu, X. A novel multi-objective competitive swarm optimization algorithm for multi-modal multi objective problems. In Proceedings of the 2019 IEEE Congress on Evolutionary Computation (CEC), Wellington, New Zealand, 10–13 June 2019; pp. 271–278. [CrossRef]
25. Li, W.; Yao, X.; Zhang, T.; Wang, R.; Wang, L. Hierarchy Ranking Method for Multimodal Multiobjective Optimization with Local Pareto Fronts. *IEEE Trans. Evol. Comput.* **2023**, *27*, 98–110. [CrossRef]
26. Liang, J.J.; Qu, B.; Gong, D.; Yue, C. *Problem Definitions and Evaluation Criteria for the CEC 2019 Special Session on Multimodal Multiobjective Optimization*; Computational Intelligence Laboratory, Zhengzhou University: Zhengzhou, China, 2019; pp. 353–370.
27. Liu, Y.; Ishibuchi, H.; Yen, G.G.; Nojima, Y.; Masuyama, N. Handling imbalance between convergence and diversity in the decision space in evolutionary multimodal multiobjective optimization. *IEEE Trans. Evol. Comput.* **2019**, *24*, 551–565.
28. Vikhar, P.A. Evolutionary algorithms: A critical review and its future prospects. In Proceedings of the 2016 International Conference on Global Trends in Signal Processing, Information Computing and Communication (ICGTSPICC), Jalgaon, India, 22–24 December 2016; pp. 261–265. [CrossRef]
29. Schutze, O.; Vasile, M.; Coello, C.A.C. Computing the set of epsilon-efficient solutions in multiobjective space mission design. *J. Aerosp. Comput. Inf. Commun.* **2011**, *8*, 53–70. [CrossRef]
30. Lin, Q.; Lin, W.; Zhu, Z.; Gong, M.; Li, J.; Coello, C.A.C. Multimodal multiobjective evolutionary optimization with dual clustering in decision and objective spaces. *IEEE Trans. Evol. Comput.* **2020**, *25*, 130–144. [CrossRef]
31. Zhou, A.; Zhang, Q.; Jin, Y. Approximating the Set of Pareto-Optimal Solutions in Both the Decision and Objective Spaces by an Estimation of Distribution Algorithm. *IEEE Trans. Evol. Comput.* **2009**, *13*, 1167–1189. [CrossRef]


**Disclaimer/Publisher's Note:** The statements, opinions and data contained in all publications are solely those of the individual author(s) and contributor(s) and not of MDPI and/or the editor(s). MDPI and/or the editor(s) disclaim responsibility for any injury to people or property resulting from any ideas, methods, instructions or products referred to in the content.